International Journal of Reliability, Risk and Safety: Theory and Application

Online ISSN: 2676-3346

OPEN ACCESS

Vol. 8/ Issue 1/ Year 2025/ pp. 89-97

DOI: 10.22034/IJRRS.2025.8.1.8

Received: 16 April 2025, Revised: 04 July 2025, Accepted: 18 July 2025

Available online at: https://www.ijrrs.com

Original Research Article

Evaluation of Radiation Shielding Reliability and Safety in Heavy Metal-Oxide-Reinforced Polyethylene Composites

Mohammadreza Alipoor * and Mahdi Eshghi

Department of Physics, Imam Hossein University, Tehran, Iran

***M.Alipoor@ihu.ac.ir**

Abstract

As a potentially hazardous factor in industrial, medical, and research environments, ionizing radiation has consistently created significant human and environmental safety and health challenges. In the present investigation, the influence of heavy element oxide deposition on the radiation shielding characteristics of high-density polyethylene is meticulously examined. This research delineates photon attenuation-related parameters, including the linear attenuation coefficient, mass attenuation coefficient, tenth-value layer, half-value layer, and radiation shielding efficiency of these materials, contextualized within the energy spectrum from gamma photons (0.015-10 MeV). To authenticate the simulation outcomes, the mass attenuation coefficient values computed via Geant4 were juxtaposed with the findings from the Phy-x program, revealing a commendable concordance between the two sets of results. The observed alignment of the data substantiates that the Geant4 tool constitutes a practical methodology for exploring gamma ray shielding properties. The findings elucidate a distinct correlation between the augmentation of heavy oxide concentration and the enhancement of radiation shielding efficacy. Furthermore, the results indicate that the radiation shielding efficiency gradually declines within the low energy spectrum, subsequently experiencing a pronounced increase. Ultimately, it underscores the influence of incorporating heavy element oxides on the efficacy of gamma-ray attenuation.

Keywords: Gamma-rays; Shielding; Polyethylene; Bismuth oxide; Geant4; Thallium oxide.

Nomenclature

MAC	Mass Attenuation Coefficient
LAC	Linear Attenuation Coefficient
HVL	Half Layer Value
TVL	Tenth Layer Value
RPE	Radiation Protection Efficiency
HDPE	High-Density Polyethylene
RD%	Relative Difference Percent

1. Instructions

Exposure to hazardous ionizing radiation can manifest across multiple domains, including nuclear power facilities, particle accelerators, industrial dosimetry, research laboratories, agricultural practices, aerospace technology, medical imaging modalities, radiotherapy, and nuclear medicine [1, 2]. Given that gamma rays and X-rays can be generated through diverse interactions such as radioactive decay from unstable isotopes, bremsstrahlung phenomena involving accelerated electrons, characteristic X-ray emissions, annihilation events, inelastic neutron scattering, and neutron absorption processes, the implementation of protective measures against these forms of radiation is of paramount significance [3]. Radiation shielding mechanisms are indispensable for mitigating radiation-related hazards and limiting exposure to acceptable thresholds. These shields operate by absorbing, diminishing, or redirecting ionizing radiation by utilizing materials with high atomic numbers. The optimization of risk assessment and protective system design augments occupational safety while concurrently promoting the sustainability of

How to cite this article:

M. Alipoor and M. Eshghi, "Evaluation of radiation shielding reliability and safety in heavy metal-oxide-reinforced polyethylene composites ," *International Journal of Reliability, Risk and Safety: Theory and Application*, vol. 8, no. 1, pp. 89-97, 2025, doi: 10.22034/IJRRS.2025.8.1.8

radioactive operations by reducing both economic liabilities and legal obligations. Lead, often selected for its efficacy in radiation protection, is notable primarily due to its elevated atomic number, substantial density, and significant attenuation coefficients, which collectively enhance interactions with high-energy photons and facilitate an effective shielding process [4]. Despite the prevalent application of lead in gamma radiation shielding, the intrinsic drawbacks associated with lead, particularly its toxicological risks and considerable mass, underscore the pressing necessity to explore and identify non-toxic alternatives that can fulfil the essential function of effective shielding materials without engendering detrimental health or environmental consequences [5, 6]. Concrete has gained prominence as a viable substitute for metallic materials in the arena of radiation shielding, particularly against radiation within the diagnostic energy spectrum, primarily attributable to its ubiquitous availability and cost-effectiveness, thereby rendering it a practical selection for numerous applications. Nevertheless, this conventional approach frequently necessitates the construction of voluminous shields, which can present challenges related to weight and spatial limitations in various contexts [7]. In this regard, contemporary research focuses on developing advanced protective materials and methodologies to enhance efficacy while minimizing mass to improve safety and address operational and economic challenges [8-10]. Metal-polymer composites represent one of the most frequently examined advanced materials employed in gamma radiation attenuation in recent years [11, 12]. Metal-polymer composites fundamentally consist of a metallic filler integrated with a polymeric matrix. The enhanced characteristics of metal-polymer composites arise from the uniform distribution of high atomic number particles within a lightweight and flexible polymer matrix. Indeed, they possess the advantage of being lightweight while offering effective radiation shielding capabilities [13]. A diverse array of alternative metallic fillers, including elements such as tungsten, boron, gadolinium, and bismuth, in conjunction with a variety of polymer composites incorporating these elements, have been meticulously identified for their potential to augment the effectiveness of radiation shielding [14, 15]. Furthermore, polymeric materials distinguished by high hydrogen content are being increasingly employed in radiation shielding applications owing to their favourable properties and performance metrics in attenuating radiation exposure [16 Appropriate amalgamations of diverse fillers, encompassing bismuth oxide, lead oxide, boron nitride, boron carbide, tungsten carbide, and gadolinium oxide, have been utilized within the polymer matrix to augment the gamma-ray attenuation efficacy, thereby improving its effectiveness in radiation shielding [17]. It is noteworthy that bismuth oxide presents a considerable advantage over conventional lead-based fillers due to its markedly reduced toxicity. Bismuth, categorized as a heavy metal, exhibits comparable shielding capabilities to lead, yet its toxicological profile is significantly less detrimental. Numerous investigations have explored the efficacy of various bismuth compounds, including bismuth oxide, bismuth carbonate, and bismuth nitrate, within X-ray shielding applications [18, 19]. Thallium is a heavy element found in several sulphide and metallic minerals; it is a byproduct of the smelting and mining sectors, coal-fired power facilities, and the cement manufacturing industry, significantly contributing to soil contamination with this element. Reintegrating this waste into the polymer production process mitigates environmental impacts and results in composites that exhibit radiation resistance [20]. Implementing industrial waste as a type of reinforcement in polymer composites shows considerable promise in the emerging field of recycled materials specifically designed for shielding applications and is an innovative approach to achieve a safe shield. This has less impact on the environment [21-23]. In addition, non-commercial industrial waste materials, often underutilized, strengthen the possibility of their integration into sustainable production practices for different radiation protection components, thus aligning with environmental protection efforts. This innovative approach highlights the material properties of polymer composites as radiation shields and contributes to the overall goal of reducing environmental impacts using industrial waste.

2. Materials and Methods

High-density polyethylene (HDPE) is a thermoplastic polymer produced from the monomer ethylene. An impressive strength-to-density ratio, exceptional chemical resistance, and remarkable versatility characterize it. Due to its inherent durability and recycling capacity, polyethylene has a wide range of applications in sectors such as packaging and various coatings. The molecular structure of this polymer is composed of extended chains of ethylene monomers—the polymerization process of ethylene results in the formation of long chains of $-CH_2-CH_2-$ units. The linear configuration of polyethylene facilitates a high degree of crystallinity (typically from 60 to 80%), which increases its density and mechanical flexibility [24, 25]. Bismuth oxide is not justified due to its toxicity and the cost of raw materials [26]. The selected polymer blend, which consists of four distinct components, including HDPE, Bi_2O_3, Tl_2O, and PbO, was chosen through a careful procedure that involved partial replacement of the bismuth oxide blend with an alternative blend, namely thallium oxide. Table 1 delineates the chemical composition and density of five distinct polymer composite samples (PC_1 to PC_5) formulated for radiation shielding. The HDPE matrix imparts flexibility and durability to the composites. Bismuth oxide is exceptionally proficient in absorbing X-rays and gamma-rays via the photoelectric effect, especially within the low-to-medium energy range (<500 keV). Its reduction

from PC_1 to PC_5 suggests a trade-off for other shielding mechanisms. Thallium oxide demonstrates effective photon attenuation at elevated energy levels, particularly through Compton scattering and pair production. Lead Oxide, fixed at 20% to maintain baseline photon shielding while testing Tl_2O efficacy. A progressive increase in density is observed, from PC_1 (5.13 g/cm³) to PC_5 (5.44 g/cm³), attributable to the increased content of Tl_2O, which possesses a greater density than Bi_2O_3.

Table 1. Chemical composition and density of polymer composite.

samples	HDPE	Bi_2O_3	Tl_2O	PbO	Density ($g.cm^{-3}$)
PC_1	50	25	5	20	5.13
PC_2	50	20	10	20	5.21
PC_3	50	15	15	20	5.28
PC_4	50	10	20	20	5.36
PC_5	50	5	25	20	5.44

2.1 Simulation Toolkit

This computational toolkit is fundamentally anchored in the core principles of Monte Carlo methodologies and is especially adept at accurately modeling and simulating intricate interactions between particles and matter. We have employed the Geant4 toolkit to conduct a comprehensive simulation that emphasizes the transport of photons during their ingress and attenuation through the polymer blend, particularly within the delineated energy range of 0.015 to 10 MeV. The primary objective of this simulation was to derive the mass attenuation coefficients pertinent to the polymer blend, which consequently facilitated the computation of additional gamma shielding parameters, including the half-value layer and the tenth-value layer. The simulation was executed utilizing a cubic box of dimensions 5 cm, containing a sample of the polymer blend by the weight fraction of the constituents specified within the simulation framework. The attenuation of photons is determined by simulating all possible physical processes for photons (such as photoelectric effects, Compton scattering, Rayleigh scattering, pair production) and bremsstrahlung, ionization, and positron annihilation for electrons and positrons. The underlying physics models are governed by Geant4, G4EMStandardPhysics_option4 package, which provides the most detailed treatment of electromagnetic interactions. This package leverages evaluated data libraries to ensure accurate cross-section calculations for each interaction process. Option 4 extends the simulation's validity to lower energies, improving precision in modeling attenuation phenomena. Each simulation tracks 1 million gamma photons to minimize statistical uncertainties, ensuring robust and reproducible results. Combining high-fidelity physics models, comprehensive cross-section data, and many simulated events enhances the shielding parameters' reliability. This approach aligns with established Monte Carlo best practices, where increased particle statistics reduce statistical errors, as demonstrated in prior studies. Using Geant4's most advanced electromagnetic physics options further validates the accuracy of the simulated interactions, making the results suitable for comparative analysis with experimental data [27, 28].

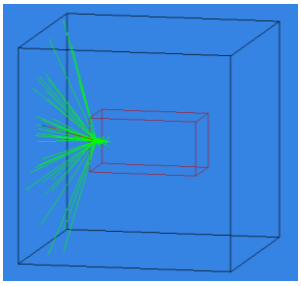

Figure 1. Geometric shape is simulated in the Geant4 simulation tool.

3. Phy-X/PSD program

The Phy-X/PSD software calculates various shielding parameters across a range of energy values. To facilitate these computations, it is imperative to provide the chemical composition of the material (weight fraction) in conjunction with its density. The assessment of shielding parameters is achievable within the photon energy spectrum of 0.015–10 MeV. This software is capable of efficiently and swiftly calculating eighteen unique protective parameters. Specific photon energy values are integrated as selectable options within the Phy-X/PSD software, given their correspondence with the energies emitted by radioactive isotopes (^{241}Am, ^{55}Fe, ^{133}Ba, ^{60}Co, ^{109}Cd, ^{132}E, ^{131}I, and ^{137}Cs) that may be employed in medical, industrial, and nuclear environments where personnel are present. The importance and validity of Phy-X/PSD simulation are given in [29]. Usually, researchers who perform experimental or simulation work try to validate their results using this software. In this way, if the deviation between the Phy-x/PSD results and the simulated data is slight, the simulated results can be validated [30, 31].

4. Results and Discussion

The mass attenuation coefficient is one of the quantities often used to investigate the penetration of photons in an absorbing material. The mass attenuation coefficient was explicitly calculated for polyethylene composites across the energy spectrum from 0.015 MeV to 10 MeV using advanced Geant4 simulation techniques, which are well-regarded for their accuracy in modeling particle interactions and transport. Furthermore, to ensure the

robustness and validity of the simulation results, data were carefully extracted from the Phy-x computational program to validate the findings obtained from the Geant4 simulation accurately. Validation of the values is essential in this work, as this parameter is used to evaluate other quantities. Comparison of the results in Table 2 showed that the difference between the theoretical values obtained from Phy-x and the simulated values via Geant4 is less than 2%, thus confirming the reliability of the current results. This difference is related to the electromagnetic models included in Geant4, which transport photons with high accuracy and report results with exceptional sensitivity.

Table 2. Comparison of data results from Geant4 and Phy-x in terms of photon energy.

Energy (MeV)	PC_1			PC_2			PC_3			PC_4			PC_5		
	Geant 4	Phy-x	±RD %	Geant4	Phy-x	±RD %	Geant4	Phy-x	±RD %	Geant 4	Phy-x	±RD %	Geant 4	Phy-x	±RD %
0.015	54.282	54.366	0.16	56.243	56.364	0.21	58.205	58.351	0.25	60.166	60.364	0.33	62.128	62.35	0.36
0.02	40.258	40.382	0.31	40.266	40.390	0.31	40.274	40.390	0.29	40.281	40.406	0.31	40.289	40.405	0.29
0.03	14.285	14.256	0.20	14.279	14.251	0.19	14.273	14.244	0.20	14.267	14.242	0.17	14.261	14.235	0.18
0.05	3.861	3.858	0.08	3.857	3.854	0.07	3.853	3.850	0.07	3.849	3.848	0.03	3.845	3.844	0.04
0.08	1.203	1.225	1.78	1.201	1.224	1.84	1.199	1.222	1.87	1.197	1.221	1.94	1.195	1.219	1.97
0.1	2.671	2.669	0.06	2.674	2.671	0.12	2.678	2.672	0.20	2.681	2.675	0.23	2.685	2.676	0.31
0.15	1.016	1.018	0.13	1.016	1.018	0.16	1.016	1.018	0.16	1.017	1.019	0.21	1.017	1.019	0.21
0.2	0.540	0.539	0.13	0.540	0.539	0.15	0.540	0.539	0.18	0.540	0.539	0.19	0.540	0.539	0.22
0.4	0.167	0.166	0.21	0.166	0.166	0.19	0.166	0.166	0.18	0.166	0.166	0.15	0.166	0.166	0.15
0.511	0.126	0.128	1.91	0.126	0.128	1.91	0.125	0.128	1.90	0.125	0.128	1.91	0.125	0.128	1.90
0.8	0.085	0.084	0.81	0.085	0.084	0.81	0.085	0.084	0.81	0.085	0.084	0.80	0.085	0.084	0.81
1.5	0.056	0.056	0.18	0.056	0.056	0.18	0.056	0.056	0.18	0.056	0.056	0.18	0.056	0.056	0.19
2	0.048	0.048	0.09	0.048	0.048	0.09	0.048	0.048	0.09	0.048	0.048	0.09	0.048	0.048	0.08
4	0.038	0.038	0.24	0.038	0.038	0.24	0.038	0.038	0.24	0.038	0.038	0.25	0.038	0.038	0.24
5	0.036	0.036	0.08	0.036	0.036	0.08	0.036	0.036	0.08	0.036	0.036	0.06	0.036	0.036	0.07
6	0.035	0.035	0.39	0.035	0.035	0.38	0.035	0.035	0.38	0.035	0.035	0.36	0.035	0.035	0.36
8	0.035	0.034	0.77	0.035	0.034	0.76	0.035	0.034	0.76	0.035	0.035	0.74	0.035	0.035	0.74
10	0.035	0.034	0.82	0.035	0.035	0.81	0.035	0.035	0.80	0.035	0.035	0.77	0.035	0.035	0.77

The changes in the calculated mass attenuation coefficient values are shown in Figure 3. Figure 3 shows a sharp increase in polyethylene composites' mass attenuation coefficient values . This increase is initially due to the rise in energy level. Most of the interaction between photons and matter occurs in the low-energy region, and here the photoelectric absorption interaction cross section is a function of atomic number ($Z^{4.5}$). The maximum attenuation values for all samples occur at 15 keV, and the attenuation decreases with increasing energy from 15 keV to 100 keV. Therefore, adding heavy element oxides increases the attenuation at low energies. The mass attenuation coefficient values increase with increasing energy up to 150 keV. However, the mass attenuation coefficient values decrease after 150 keV due to the linear dependence between the atomic number of the material and the Compton scattering cross section. This decrease continues until all polyethylene composites' mass attenuation coefficient values become almost constant. However, the mass attenuation coefficient values register small increases in the high-energy region because the pair production process becomes dominant with increasing energy, as the cross section of this interaction is related to the square of the atomic number at higher energies. Several factors influence the mass attenuation coefficient values. Among these factors are the chemical composition of the polyethylene composites, the atomic numbers, and the energy level considered adequate. For the latter, we have a different interaction resulting from the interaction between energy and material. The chemical structure of the polyethylene composites is also a fundamental parameter that influences the mass attenuation coefficient values. For example, adding elements with higher and closer K absorption edges than any other element affects the mass attenuation coefficient values.

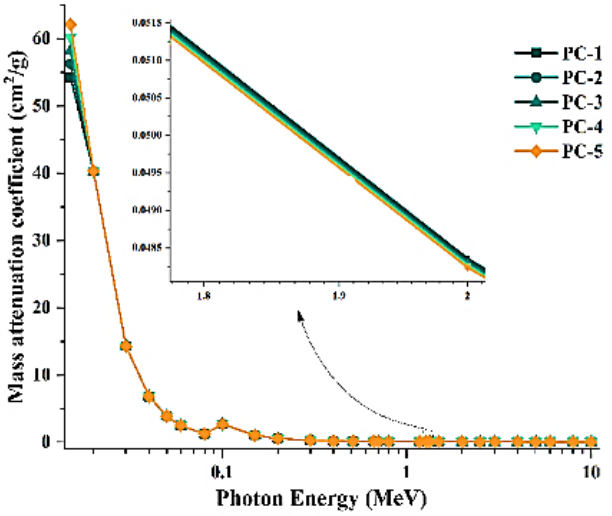

Figure 3. Mass attenuation coefficient in terms of photon energy.

The linear attenuation coefficient (LAC) and the mass attenuation coefficient (MAC) are primary quantities used to evaluate various materials' shielding properties and performance. The linear attenuation coefficient values are related to the photon energy range of 0.015 to 10 MeV and are shown in Figure 4. It is important to note that the linear attenuation coefficient is directly proportional to the photon energy level. The linear attenuation coefficient experiences a significant decrease at energies below 0.1 MeV, indicating that the effect of elements with high atomic numbers on attenuation decreases as the photoelectric effect decreases. Given the relative closeness of the densities, the results show a clear trend: materials with higher densities are associated with higher levels of the linear attenuation coefficient. The probability of pair production scales approximately as Z^2. Tl_2O high-Z composition significantly boosts the pair production cross-section compared to lower-Z constituents in other blends at high energies. The high density of Tl_2O provides more target nuclei per unit volume, further amplifying pair production events. Our simulations show that PC_5 exhibits ~25% higher pair production rates at 10 MeV than blends without Tl_2O. The 511 keV photons generated from positron annihilation are reabsorbed efficiently via photoelectric effect (due to Tl's high-Z) and Compton scattering, creating a "cascade attenuation" effect. Tl's high electron density increases the probability of positron annihilation-in-flight, reducing high-energy bremsstrahlung emissions that could otherwise degrade shielding performance. Although the material density does not change significantly in the enlarged section, the PC-5 sample shows superior attenuation properties compared to the other selected samples.

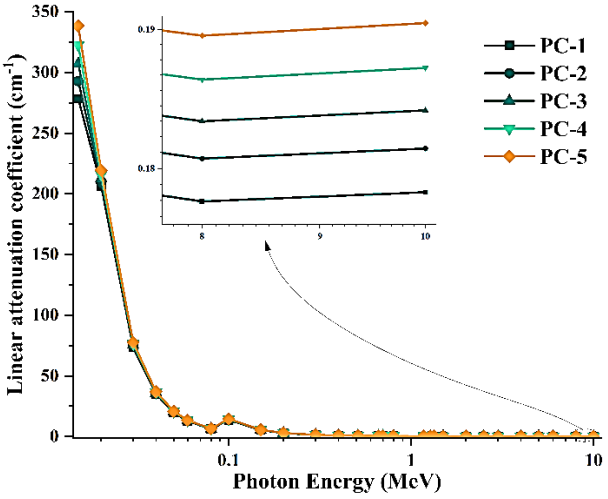

Figure 4. Linear attenuation coefficient in terms of photon energy.

The half-value layer is another quantity that plays a significant role in evaluating photonic shielding properties. The half-value layer is defined as the thickness of a given material that can reduce exactly half of the incident photon intensity. Figure 5 shows the half-value layer (HVL) for the samples in the selected energy range. Furthermore, a thinner half-value layer indicates better radiation shielding capabilities. From Figure 5, the half-value layer values tend to increase with increasing energy levels.

In contrast, the half-value layer value at energies of 0.511 and 0.662 MeV does not show much difference; with increasing energy, the difference in the half-value layer thickness is clear. The performance of PC_5 is significantly better compared to the other selected materials. This effect is related to the unique properties of absorbing materials and the interactions of photons with the absorbing material.

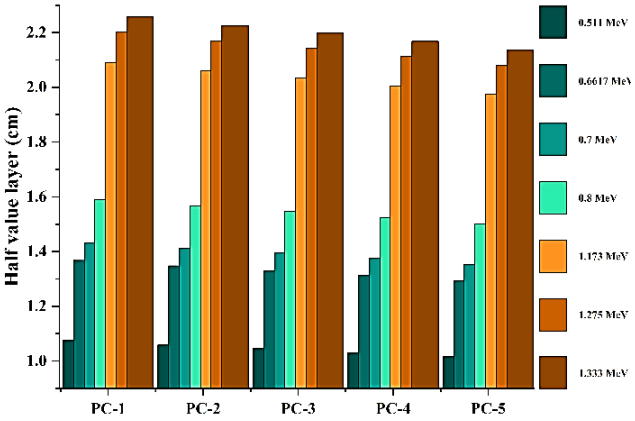

Figure 5. Half-value layer for selected energy

Figure 6 shows the values of the tenth-value layer for a range of different samples studied in the energy range of 0.015 to 10 MeV. Furthermore, Figure 6 shows that the shielding materials composed of PC_5 exhibit superior ability to reduce gamma rays, while requiring a

smaller overall shielding thickness. In the enlarged section, the absorption edge effect is well demonstrated. For low-energy photons (0.1–0.3 MeV), the tenth value layer (TVL) decreases due to the predominance of the photoelectric effect, which is highly efficient in high-Z materials such as Bi_2O_3 and PbO within the composites. For medium-energy photons (0.3–0.8 MeV), the TVL increases as Compton scattering becomes the dominant interaction mechanism, reducing overall attenuation efficiency. At high energies (>0.8 MeV), the TVL may plateau or continue rising due to pair production requiring higher energies. PC-1 demonstrates superior performance at low energies, where the photoelectric effect dominates, while PC-5 excels at high energies, benefiting from pair production and density effects. Including thallium oxide is crucial for effective shielding against high-energy photons, while bismuth enhances low-energy attenuation.

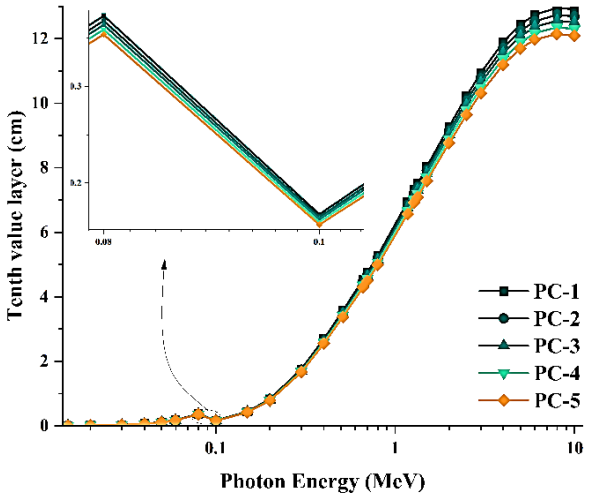

Figure 6. Tenth layer value in terms of photon energy

Figure 7 illustrates the radiation attenuation efficiency (RPE) of selected polymer samples as a function of photon energy, offering key insights into the photon absorption performance of these materials. The RPE quantifies the ratio of absorbed photons to the total incident photons, and as shown in the figure, it decreases significantly with increasing photon energy. This decline is attributed to the greater penetrability of high-energy photons, which results in deeper penetration and a reduction in the absorbed photon fraction ($I_0 - I_t$). At energies below 100 keV, the RPE approaches 100%, indicating near-total attenuation. However, as energy rises beyond 100 keV, efficiency drops sharply. In the intermediate energy range, the increased probability of Compton scattering elevates the transmitted photon flux, further reducing attenuation efficiency. Above 1 MeV, the rate of decline slows, and by 4 MeV, the efficiency stabilizes at a nearly constant level.

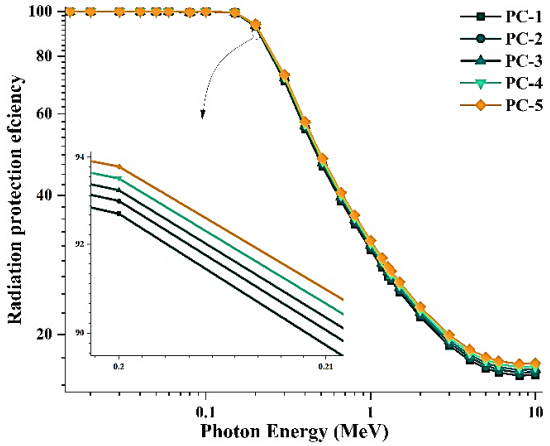

Figure 7. Radiation protection efficiency in terms of photon energy

The values of radiation protection efficiency for polyethylene composites at 1 and 2 cm thicknesses are shown in Figure 7. According to the figure, the radiation attenuation efficiency of polyethylene composites increased with increasing sample thickness. This provides a clear understanding of how the material thickness affects the gamma ray attenuation characteristics. The path length of photons increases in samples with greater thickness, leading to more photon-electron interactions. It should be noted that the values of radiation attenuation efficiency increase continuously and gradually as the glass thickness increases from 1 to 2 cm. Thickness is an important factor, especially when considering space constraints, to determine the effectiveness of a radiation shield. With increasing thickness, the values of radiation attenuation efficiency increased from 29 to 38% at an energy of 511 keV for the selected samples. Also, increasing the thickness increased the radiation attenuation efficiency values from 54 to 61% at 662 keV energy for the samples. Notably, the RPE exhibits a steady and gradual rise as thickness increases from 1 cm to 2 cm, confirming that thickness is a critical factor—particularly when optimizing shield effectiveness under weight and location constraints.

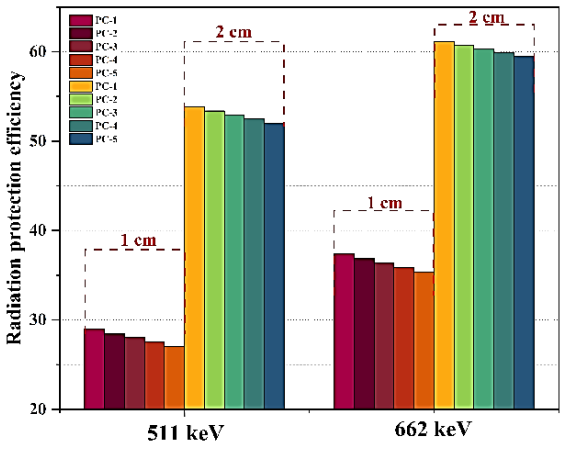

Figure 8. Radiation attenuation efficiency as a function of thickness for energies of 511 and 662 keV.

Lead Equivalent Thickness denotes the thickness of lead that yields an identical degree of radiation attenuation as a specified material. This metric juxtaposes the shielding efficacy of various materials against lead. It is utilized as a benchmark due to its substantial density and atomic number, rendering it an exemplary radiation absorber. Figure 9 presents the lead equivalent thickness of five polymer samples (PC_1 to PC_5) at 0.511, 0.662, 1.173, 1.275, and 1.333 MeV photon energy. The data shows a clear increasing trend in shielding effectiveness, with values rising from 0.51 cm for PC_1 to 1.333 cm for PC_5. The lead equivalent thickness increases consistently across the samples, indicating enhanced photon attenuation capabilities. PC_5 has the highest shielding performance, with a lead equivalence of 2.6 times greater than PC_1. The results are reported for a defined photon energy, which is critical because shielding efficiency varies with energy. The ascending lead equivalent thickness from PC_1 to PC_5 underscores the potential of engineered polymers as next-generation radiation shields. By leveraging high-Z additives and density modulation, these materials achieve performance comparable to lead while offering advantages like flexibility and reduced toxicity.

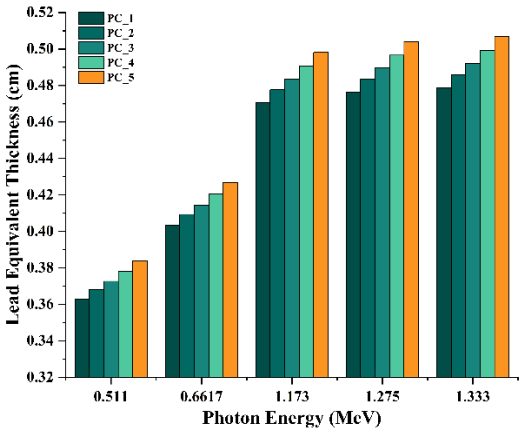

Figure 9. Equivalent lead thickness for samples, depending on the selected energy

The elucidation of findings about the fast neutron removal cross-section is paramount within the domain of radiation physics, particularly concerning neutron shielding, reactor architecture, and radiation safety protocols. The Fast Neutron Removal Cross-Section (FNRCS) is a measure of a material's ability to attenuate fast neutrons (typically with energies > 0.1 MeV) through scattering and absorption processes. The fast neutron removal cross-section (Σ_R) delineates the likelihood per unit path length of a fast neutron being extricated from the principal beam because of interactions encompassing elastic scattering, inelastic scattering, or nuclear reactions. Fast neutrons hold significant importance in radiation protection and dosimetry due to their substantial contribution to radiation doses, their pronounced penetration capabilities, and their propensity to engender secondary particles, including recoil protons or gamma rays. The removal cross-section quantifies the reduction of fast neutrons in shielding materials, essential for compliance with radiation safety standards. Figure 9 presents the FNRCS values for polymer samples (PC-1 to PC-5) loaded with thallium oxide. The FNRCS values range from 0.36 cm^{-1} to 0.385 cm^{-1}, indicating a gradual increase in neutron shielding efficiency across the samples. The upward trend suggests that incorporating thallium oxide into the host polymer significantly enhances its ability to attenuate fast neutrons, as evidenced by the rising FNRCS values. The consistent rise in values from PC_1 to PC_5 implies a potential correlation between the concentration of thallium oxide and the shielding performance. When an energetic neutron collides with a heavy nucleus, it loses some energy (inelastic scattering) or changes direction (elastic scattering). These processes help reduce the neutron's energy and ultimately absorb it. Thallium isotopes (^{203}Tl and ^{205}Tl) have a significant neutron absorption cross-section. After the neutrons are reduced in energy by scattering, their probability of being absorbed by thallium nuclei increases. Hydrogen-rich polymers (such as polyethylene) convert fast neutrons into thermal neutrons, while thallium absorbs these slowed neutrons.

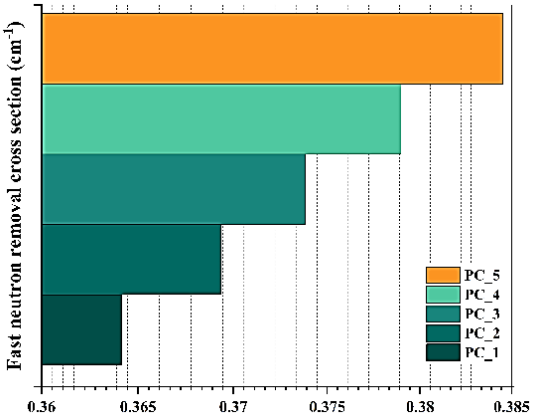

Figure 10. The Fast neutron removal cross-section for samples

Table 3 data reveal distinct neutron interaction behaviors and provide critical insights into radiation shielding mechanisms.

Elastic scattering cross-section ($\sigma_{elastic}$): This represents the probability of neutrons colliding with an atomic nucleus and changing direction without energy loss. The values remain stable around 0.25 cm^2/g but slightly decrease from PC_1 (0.25213 cm^2/g) to PC_5 (0.24937 cm^2/g). This minor decline may stem from variations in polymer density or structure, though its impact on overall shielding performance is negligible.

Absorption cross-section (σ_{abs}) indicates the likelihood of neutron absorption by nuclei. A linear increase is observed from PC_1 (0.6483×10^{-5} cm^2/g) to PC_5 (1.4389×10^{-5} cm^2/g), suggesting the incorporation of neutron-absorbing (H ،C ،O) into the polymer matrix.

Inelastic scattering cross-section ($\sigma_{inelastic}$): Neutrons transfer part of their energy to nuclei. This cross-section also exhibits a linear increase, rising from PC_1 (3.2095 × 10^{-5} cm^2/g) to PC_5 (7.3721 × 10^{-5} cm^2/g). Heavier samples (e.g., PC_5) are more effective in neutron energy reduction due to enhanced inelastic interactions.

Total cross-section (σ_{total}): This combined metric shows a marginal decrease from PC_1 (0.25245 cm^2/g) to PC_5 (0.25012 cm^2/g). Despite the rising absorption and inelastic scattering contributions, the slight dip in elastic scattering slightly lowers the overall value.

Table 3. Total cross-section of the polymer samples for neutron attenuation.

Sample	total neutron cross section (cm^2/g)			
	$\sigma_{elastic}$	σ_{abs} ($\times 10^{-5}$)	$\sigma_{Inelastic}$ ($\times 10^{-5}$)	σ_{total}
PC_1	0.25213	0.6483	3.2095	0.25245
PC_2	0.25144	0.8461	4.2374	0.25187
PC_3	0.25075	1.0436	5.2565	0.25129
PC_4	0.25006	1.2413	6.2931	0.2507
PC_5	0.24.937	1.4389	7.3721	0.25012

The compositional variation from PC_1 to PC_5 demonstrates a strategic shift from bismuth-dominated photon shielding to thallium-enhanced neutron-photon hybrid shielding. PC_5, with its high Tl_2O content and elevated density, emerges as the optimal choice for high-energy radiation environments, offering superior shielding performance. PC_1, in contrast, remains highly effective for low-energy radiation applications due to its composition. While Tl_2O offers superior shielding performance, its toxicity necessitates stringent handling and encapsulation.

5. Conclusion

This study investigated polyethylene-based polymer composites with heavy element oxides for their radiation shielding properties. The primary objective was to evaluate the effect of increasing the heavy element oxide on these materials commonly used for photon shielding. The comparison included assessing the percentage change in key parameters, including density, linear attenuation coefficient, mass attenuation coefficient, half-value layer, tenth-value layer, and radiation shielding efficiency, after adding heavy element oxides. In particular, the linear attenuation coefficient and mass attenuation coefficient were increased. These significant improvements emphasize the effectiveness of heavy element oxides as an additive in increasing the capacity to absorb photons. The results demonstrate that enhanced photon absorption improves gamma-ray shielding performance with increased material thickness. Notably, PC_5 exhibits superior shielding efficiency across all energies (0.015 to 15 MeV), attributed to its optimal composition of Tl_2O (providing high-Z elements for effective attenuation) and balanced polymer matrix. The mass attenuation coefficient (MAC) analysis reveals energy-dependent trends, with higher MAC values at lower energies, emphasizing the materials' enhanced shielding capability for diagnostic-range X-rays. The Tl_2O dominance in MAC performance further underscores its critical role in radiation protection. These findings highlight the potential of PC_5 composites as lightweight, flexible alternatives to conventional shielding materials. These findings position polyethylene-based polymers with heavy element oxides as next-generation materials capable of meeting increasingly stringent radiation safety requirements in fields such as medical facilities, nuclear power plants, space exploration, industrial applications, and research laboratories, while also responding to the growing demand for non-toxic, high-performance shielding solutions. Future work could focus on optimizing the samples by an ANN model to increase absorption and attenuation, for application over a broader range of energies and locations.

Conflict of Interests

No conflict of interest has been expressed by the authors.

6. References

[1] M. A. Hill, "The variation in biological effectiveness of X-rays and gamma rays with energy," *Radiation Protection Dosimetry*, vol. 112, no. 4, pp. 471–481, 2004, https://doi.org/10.1093/rpd/nch091

[2] U. A. Tarim, E. N. Ozmutlu, S. Yalcin, O. Gundogdu, D. A. Bradley, and O. Gurler, "Evaluation of gamma-ray attenuation properties of bismuth borate glass systems using Monte Carlo method," *Radiation Physics and Chemistry*, vol. 140, pp. 403–405, 2017, https://doi.org/10.1016/j.radphyschem.2017.03.031.

[3] M. S. Al-Buriahi, H. Arslan, H. O. Tekin, V. P. Singh, and B. T. Tonguc, "MoO_3-TeO_2 glass system for gamma ray shielding applications," *Materials Research Express*, vol. 7, no. 2, 2020, Art. no. 025202, https://doi.org/10.1088/2053-1591/ab6db4.

[4] M. Erdem, O. Baykara, M. Doğru, and F. Kuluöztürk, "A novel shielding material prepared from solid waste containing lead for gamma ray," *Radiation Physics and Chemistry*, vol. 79, no. 9, pp. 917–922, 2010, https://doi.org/10.1016/j.radphyschem.2010.04.009.

[5] Y. S. Rammah et al., "Investigations on borate glasses within SBC-Bx system for gamma-ray shielding applications," *Nuclear Engineering and Technology*, vol. 53, no. 1, pp. 282–293, 2020, https://doi.org/10.1016/j.net.2020.06.034.

[6] N. J. AbuAlRoos, N. A. B. Amin, and R. Zainon, "Conventional and new lead-free radiation shielding materials for radiation protection in nuclear medicine: A review," *Radiation Physics and Chemistry*, vol. 165, 2019, Art. no. 108439, https://doi.org/10.1016/j.radphyschem.2019.108439.

[7] E. Şakar, Ö. F. Özpolat, B. Alım, M. I. Sayyed, and M. Kurudirek, "Phy-X / PSD: Development of a user friendly online software for calculation of parameters relevant to radiation shielding and dosimetry," *Radiation Physics and*

Chemistry, vol. 166, 2019, Art. no. 108496, https://doi.org/10.1016/j.radphyschem.2019.108496.

[8] A. M. El-Khatib et al., "Enhancement of Bentonite Materials with Cement for Gamma-Ray Shielding Capability," *Materials*, vol. 14, no. 16, 2021, Art. no. 4697, https://doi.org/10.3390/ma14164697.

[9] A. M. El-Khatib, T. I. Shalaby, A. Antar, and M. Elsafi, "Improving gamma ray shielding behaviors of polypropylene using PBO nanoparticles: an experimental study," *Materials*, vol. 15, no. 11, p. 3908, May 2022, https://doi.org/10.3390/ma15113908.

[10] E. Burgio, P. Piscitelli, and L. Migliore, "Ionizing Radiation and Human Health: Reviewing models of exposure and mechanisms of cellular damage. An Epigenetic perspective," *International Journal of Environmental Research and Public Health*, vol. 15, no. 9, p. 1971, 2018, https://doi.org/10.3390/ijerph15091971.

[11] M.R. Alipoor and M. Eshghi, "Gamma-ray Shielding Capacity of Ceramics Tb and Fe Doped with $Y_2Zr_2O_7$," *Advanced Ceramics Progress*, vol. 10, no. 1, p. 1-10, 2024, https://doi.org/10.30501/acp.2024.428521.1140.

[12] M. Ramadan, M. Kohail, A. A. Abadel, Y. R. Alharbi, R. Tuladhar, and A. Mohsen, "De-aluminated metakaolin-cement composite modified with commercial titania as a new green building material for gamma-ray shielding applications," *Case Studies in Construction Materials*, vol. 17, 2022, Art. no. e01344, https://doi.org/10.1016/j.cscm.2022.e01344. .

[13] A. Bijanu et al., "Metal-polymer composites for radiation protection: a review," *Journal of Polymer Research*, vol. 28, no. 10, 2021, https://link.springer.com/article/10.1007/s10965-021-02751-3.

[14] S. Alanazi, M. Y. Hanfi, M. W. Marashdeh, M. J. Aljaafreh, and K. A. Mahmoud, "Impact of heavy metal waste on gamma ray shielding performance of epoxy resin: an experimental investigation," *Polymer Bulletin*, vol. 81, no. 13, pp. 11729–11748, 2024, https://doi.org/10.1007/s00289-024-05273-2.

[15] C. Zeng et al., "Development of Polymer composites in radiation shielding Applications: A review," *Journal of Inorganic and Organometallic Polymers and Materials*, vol. 33, no. 8, pp. 2191–2239, 2023, https://doi.org/10.1007/s10904-023-02725-6.

[16] H. Oğul et al., "Gamma and Neutron Shielding Parameters of Polyester-based composites reinforced with boron and tin nanopowders," *Radiation Physics and Chemistry*, vol. 201, 2022, Art. no. 110474, https://doi.org/10.1016/j.radphyschem.2022.110474.

[17] Ambika et al., "Preparation and characterisation of Isophthalic-Bi_2O_3 polymer composite gamma radiation shields," *Radiation Physics and Chemistry*, vol. 130, pp. 351–358, 2016, https://doi.org/10.1016/j.radphyschem.2016.09.022.

[18] C. V. More, Z. Alsayed, Mohamed. S. Badawi, Abouzeid. A. Thabet, and P. P. Pawar, "Polymeric composite materials for radiation shielding: a review," *Environmental Chemistry Letters*, vol. 19, no. 3, pp. 2057–2090, 2021, https://doi.org/10.1007/s10311-021-01189-9.

[19] H. Alavian and H. Tavakoli-Anbaran, "Study on gamma shielding polymer composites reinforced with different sizes and proportions of tungsten particles using MCNP code," *Progress in Nuclear Energy*, vol. 115, pp. 91–98, 2019, https://doi.org/10.1016/j.pnucene.2019.03.033.

[20] A. Vaněk et al., "Thallium isotopes in metallurgical wastes/contaminated soils: A novel tool to trace metal source and behavior," *Journal of Hazardous Materials*, vol. 343, pp. 78–85, 2017, https://doi.org/10.1016/j.jhazmat.2017.09.020.

[21] H. Li et al., "Simultaneous removal of thallium and chloride from a highly saline industrial wastewater using modified anion exchange resins," *Journal of Hazardous Materials*, vol. 333, pp. 179–185, 2017, https://doi.org/10.1016/j.jhazmat.2017.03.020.

[22] B. Karbowska, "Presence of thallium in the environment: sources of contamination, distribution and monitoring methods," *Environmental Monitoring and Assessment*, vol. 188, 2016, Art. no. 640, https://doi.org/10.1007/s10661-016-5647-y

[23] J. Liu et al., "Thallium isotopic fractionation in industrial process of pyrite smelting and environmental implications," *Journal of Hazardous Materials*, vol. 384, 2019, Art. no. 121378, https://doi.org/10.1016/j.jhazmat.2019.121378.

[24] S. T. Schwab, M. Baur, T. F. Nelson, and S. Mecking, "Synthesis and deconstruction of polyethylene-type materials," *Chemical Reviews*, vol. 124, no. 5, pp. 2327–2351, 2024, https://doi.org/10.1021/acs.chemrev.3c00587.

[25] J. E. Mark Ed., *Physical Properties of Polymers Handbook*, New York: Springer, 2007, https://doi.org/10.1007/978-0-387-69002-5.

[26] B. Divband, Z. H. Al-Qaim, F. H. Hussein, D. Khezerloo, and N. Gharehaghaji, "Comparison of X-Ray Attenuation Performance, Antimicrobial Properties, and Cytotoxicity of Silicone-Based Matrices Containing Bi_2O_3, PbO, or Bi_2O_3/PbO Nanoparticles," Journal of Biomedical Physics and Engineering, vol. 14, no. 6, pp. 533-546, 2024, https://doi.org/10.31661/jbpe.v0i0.2403-1736.

[27] M.R. Alipoor, M. Eshghi, "Simulation and extraction Protective properties of bismuth-based heterojunction Nanocomposites for shielding against gamma rays." *Nano World,* vol. 20, no. 74, pp. 26-34, 2024, (in Persian).

[28] P. T. C. Lai, V. H. Hai, and N. T. T. Phuc, "Impacts of Geant4 hadronic physics models on secondary particle productions in proton therapy simulations," *Radiation Physics and Chemistry*, vol. 229, 2024, Art. no. 112451, https://doi.org/10.1016/j.radphyschem.2024.112451.

[29] A. M. El-Khayatt, "Calculation of gamma-ray attenuation parameters for local rocks," *Radiation Physics and Chemistry*, vol. 165, 2019, Art. no. 108496, https://doi.org/10.1016/j.radphyschem.2024.112451.

[30] Y. S. Alajerami et al., "Author Correction: Comprehensive study for radiation shielding features for Bi_2O_3–B_2O_3–ZnO composite using computational radioanalytical Phy-X/PSD, MCNP5, and SRIM software," *Scientific Reports*, vol. 15, 2025, Art. no. 4527, https://doi.org/10.1038/s41598-025-88060-x.

[31] M. R. Alipoor, "Enhancing gamma-ray shielding performance of HDPE composites using PbO and Bi_2O_3 reinforcements," *Journal of the Korean Physical Society,* vol. 87, pp. 243–253, 2025, https://doi.org/10.1007/s40042-025-01405-7.